

DETECTION OF He II REIONIZATION IN THE SDSS QUASAR SAMPLE

TOM THEUNS^{1,2}, MARIANGELA BERNARDI^{3,4}, JOSHUA FRIEMAN^{4,5}, PAUL HEWETT¹, JOOP SCHAYE⁶, RAVI K. SHETH^{7,5} AND MARK SUBBURAO⁴

Draft version October 25, 2018

ABSTRACT

The expansion of the Universe leads to a rapid drop in the hydrogen Ly α effective optical depth of the intergalactic medium (IGM), $\bar{\tau}_{\text{eff}} \propto (1+z)^{3.8}$, between redshifts 4 and 3. Measurements of the temperature evolution of the IGM and of the He II opacity both suggest that He II reionizes in this redshift range. We use hydrodynamical simulations to show that the observed temperature increase associated with He II reionization leads to a relatively sudden decrease in $\bar{\tau}_{\text{eff}}$ around the reionization epoch of ≈ 10 per cent. We find clear evidence for such a feature in the evolution of $\bar{\tau}_{\text{eff}}$ determined from a sample of ~ 1100 quasars obtained from the SDSS. He II reionization starts at redshift ≈ 3.4 , and lasts for $\Delta z \approx 0.4$. The increase in the IGM temperature also explains the widths of hydrogen absorption lines as measured in high-resolution spectra.

Subject headings: cosmology: observations — cosmology: theory — galaxies: formation — intergalactic medium — quasars: absorption lines

1. INTRODUCTION

Neutral hydrogen in the intergalactic medium (IGM) resonantly scatters the flux blueward of the hydrogen Ly α emission line in quasar spectra (Gunn & Peterson 1965; Bahcall & Salpeter 1965; Peebles 1993, §23). The fact that not all the flux is absorbed implies that the IGM is very highly ionized. The neutral fraction is determined from the balance between photo-ionizations, produced by the UV-background radiation from galaxies and quasars, and recombinations. For hydrogen, the recombination rate depends on temperature $\propto 1/T^{0.7}$, and so an increase in temperature will lead to a decrease in the level of absorption. Recent evidence suggests that He II reionizes around a redshift $z \sim 3\text{--}3.5$, and the associated temperature increase should have a measurable effect on the mean absorption. In this letter, we compute the optical depth evolution of a simulation in which He II reionization heats the IGM at redshift 3.4. The resulting dip in the evolution of the mean absorption matches that recently measured by Bernardi et al. (2002) in the Sloan Digital Sky Survey (SDSS) data.

Hydrodynamical simulations have proved to be very successful in reproducing many properties of the observed absorption (Cen et al. 1994; Zhang, Anninos & Norman 1995; Miralda-Escudé et al. 1996; Mückel et al. 1996; Hernquist et al. 1996; Theuns et al. 1998; Machacek et al. 2000; see e.g. Efstatouli, Schaye and Theuns (2000) for a recent review). Most of the absorption at redshifts 2–5 arises in modestly over- and under dense filamentary and sheetlike structures, leading to a forest of Ly α -absorption lines in the spectra of quasars (Lynds 1971). These structures can be described and understood with simple physical models in which the typical size of the absorbers is determined by the Jeans length of the photo-heated gas (Bi & Davidsen 1997; Schaye 2001). Given that these hydrodynamical simulations reproduce the data in great detail, we are con-

fident that they will also allow us to investigate the effect of a sudden increase in T on the mean absorption.

Several lines of recent evidence suggest that He II reionizes around $z \sim 3\text{--}3.5$, significantly later than hydrogen. Observations of the He II Ly α -forest detect a sudden increase in the mean He II opacity around $z \sim 3$ (Reimers et al. 1996; Heap et al. 2000; Kriss et al. 2001; Smette et al. 2002). Such a rapid increase in the flux of He II ionizing photons is expected to occur at the final stages of reionization when individual He III bubbles around sources percolate (Gnedin 2000). The resulting hardening of the ionizing background could be responsible for the observed jump in the relative abundance of CIV/SiIV (Songaila & Cowie 1996), although more recent data (Kim et al. 2002) apparently do not seem to support such a change (see also Davé et al. 1998). Finally, entropy injection associated with He II reionization will increase the temperature of the IGM (Miralda-Escudé & Rees 1994), which has the effect of making the Ly α -absorption lines broader on average. The gas will become nearly isothermal when the change in temperature is large. Schaye et al. (2000) detected both signatures in high-resolution Keck data, using a method based on the finding of Schaye et al. (1999; see also Ricotti et al. 2000 and Bryan & Machacek 2000) that the variation of the widths of the absorption lines as a function of column density, can be used to measure the temperature as a function of the density. Theuns et al. (2002a) performed a wavelet analysis of the spectra of several high resolution QSO spectra, and found that the data required a large increase in T by a factor ~ 2 around $z \sim 3.3$, consistent with late He II reionization (Miralda-Escudé & Rees 1994). The temperature decrease after $z \sim 3.3$ is also consistent with this interpretation (Theuns et al. 2002b). Other heating mechanisms have been discussed in the literature as well, for example galactic winds (Cen & Bryan 2001). Although these may have

¹Institute of Astronomy, Madingley Road, Cambridge CB3 0HA, UK

²Universitaire Instelling Antwerpen, Universiteitsplein 1, B-2610 Antwerpen, Belgium

³Department of Physics, Carnegie Mellon University, 5000 Forbes Ave. Pittsburgh, PA 15213

⁴University of Chicago, Astronomy and Astrophysics Center, 5640 S. Ellis Ave., Chicago, IL 60637

⁵Fermi National Accelerator Laboratory, P.O. Box 500, Batavia, IL 60510

⁶School of Natural Sciences, Institute for Advanced Study, Einstein Drive, Princeton NJ 08540

⁷Department of Physics and Astronomy, University of Pittsburgh, Pittsburgh, PA 15620

contributed to the entropy of the high redshift gas, it seems unlikely they could result in a sudden change of temperature as seems required by the data.

In the next section, we use hydrodynamical simulations to investigate the effect of He II reionization on the evolution of the mean effective optical depth, $\bar{\tau}_{\text{eff}}$. Section 3 summarizes the method used by Bernardi et al. (2002) to measure $\bar{\tau}_{\text{eff}}(z)$ from a sample of 1061 SDSS quasar spectra, and section 4 compares the data to the simulations.

2. HYDRODYNAMICAL SIMULATIONS

We will use hydrodynamical simulations to compute the change in the effective optical depth $\bar{\tau}_{\text{eff}}$, i.e. the ratio between the observed and emitted fluxes in the Ly α -forest region of a quasar spectrum,

$$\exp(-\bar{\tau}_{\text{eff}}) \equiv \left\langle \frac{F_{\text{observed}}}{F_{\text{emitted}}} \right\rangle = \langle \exp(-\tau) \rangle, \quad (1)$$

as the temperature increases during He II reionization. The Gunn-Peterson optical depth τ_{GP} of a uniform IGM at redshift z is (see Peebles 1993, §23)

$$\tau_{\text{GP}}(z) = \frac{\sigma_0 c x n_{\text{H}}}{H(z)}, \quad (2)$$

where $\sigma_0 = (3\pi\sigma_T/8)^{1/2}f\lambda_0$, with σ_T the Thomson cross-section, and $f = 0.416$ and $\lambda_0 = 1215.67\text{\AA}$ the oscillator strength and wavelength of the hydrogen Ly α -transition. The Hubble constant is $H(z)$, $x = n_{\text{H}}/n_{\text{H}}$ is the neutral fraction, and n_{H} is the hydrogen number density. In photo-ionization equilibrium,

$$x \approx (1 + x_{\text{He II}} + 2x_{\text{He III}}) \frac{n_{\text{H}}\alpha(T)}{\Gamma}, \quad (3)$$

where $x_{\text{He II}} = n_{\text{He II}}/n_{\text{H}}$ and $x_{\text{He III}} = n_{\text{He III}}/n_{\text{H}}$ are the abundances of singly and doubly ionized helium, $\alpha \approx 3.975 \times 10^{-13}(T/10^4\text{K})^{-0.7}\text{cm}^3\text{s}^{-1}$ is the hydrogen recombination coefficient, and Γ is the photo-ionization rate. We have assumed the gas to be highly ionized, $x \ll 1$. Inserting numerical values, and assuming a helium abundance of $Y = 0.24$ by mass,

$$\begin{aligned} \tau_{\text{GP}} &= 0.76 \left(\frac{\Omega_m}{0.3} \right)^{-1/2} \left(\frac{h}{0.65} \right)^{-1} \left(\frac{T}{10^4\text{K}} \right)^{-0.7} \left(\frac{\Gamma}{10^{-12}\text{s}^{-1}} \right)^{-1} \\ &\quad \left(\frac{\Omega_b h^2}{0.02} \right)^2 \left(\frac{1+z}{4} \right)^{4.5}, \end{aligned} \quad (4)$$

where $\Omega_b h^2$ is the baryon density, Ω_m the matter density, and $H_0 = 100\text{km s}^{-1}\text{Mpc}^{-1}$ is the current Hubble constant. Since the IGM is not uniform, the optical depth will fluctuate, and the resulting fluctuating Gunn-Peterson absorption produces the Ly α -forest. This is what is computed in the simulations. Because of the temperature dependence of the optical depth, we would naively expect $\bar{\tau}_{\text{eff}}$ to decrease by $\approx 1/g^{0.7}$ as the temperature increases by a factor g during He II reionization. We will show that the decrease is in fact less than that.

We have performed a simulation of a vacuum energy dominated, cosmologically flat cold dark matter model, with cosmological parameters $(\Omega_m, \Omega_b h^2, h, \sigma_8, Y) = (0.3, 0.019, 0.65, 0.9, 0.24)$. The simulations are performed using a modified version of HYDRA (Couchman, Thomas & Pearce 1995; Theuns et al. 1998), in which

the gas is photo-heated by an imposed uniform UV-background which evolves with redshift and reionizes H I and He I at $z \sim 6$ and He II at $z \sim 3.4$. During reionization of both H I and He II we artificially increase the photo-heating rates – i.e. the mean energy associated with each photo-ionization – to mimic the effects of radiative transfer (Abel & Haehnelt 1999). The temperature at the mean density, $T(z)$, of the simulation fits the data of Schaye et al. (2000) and Theuns et al. (2002a), in particular there is a sudden increase in T at $z \sim 3.4$ by a factor $g \approx 1.8$ as a result of He II reionization. Non-equilibrium rates for photo-ionization, cooling and heating are computed using the fits in Theuns et al. (1998). The particle masses for dark matter and gas are 1.1×10^7 and $2.0 \times 10^6 M_{\odot}$ respectively, and the simulation box is $12h^{-1}$ (co-moving) Mpc on a side. To illustrate the effect of He II reionization on $\bar{\tau}_{\text{eff}}$, we use a similar simulation in which He II reionization starts slightly later, at $z \sim 3.2$. Note that these simulations assume that the radiation field is spatially uniform at all times, see Sokasian, Abel & Hernquist (2002) for a He II reionization simulation that includes some radiative transfer effects.

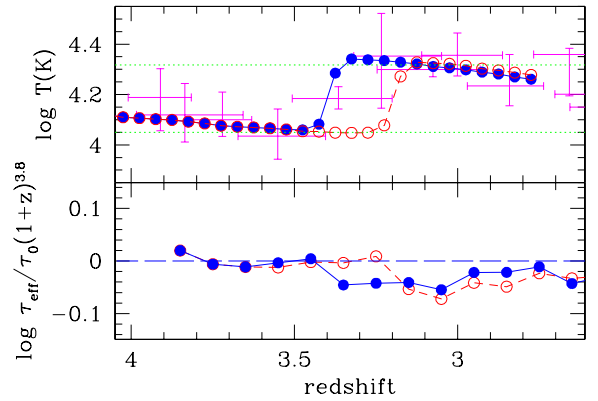


FIG. 1.— Evolution of the temperature at the mean density T (top panel), and the deviation of the effective optical depth $\bar{\tau}_{\text{eff}}$ from a power-law (bottom panel) for simulations in which He II reionization starts at $z \approx 3.4$ (full line and filled circles) and $z \approx 3.2$ (dashed line and open circles). Data points with error bars are the measurements from Schaye et al. (2000). He II reionization increases T by a factor ~ 1.8 (dotted lines). Away from reionization, $\bar{\tau}_{\text{eff}} \propto (1+z)^{\zeta}$, with $\zeta \approx 3.8$. The increase in T during reionization decreases the neutral hydrogen fraction and hence also the mean absorption. This causes $\bar{\tau}_{\text{eff}}$ to fall below the power law evolution, producing a feature in $\bar{\tau}_{\text{eff}}/(1+z)^{\zeta}$ that is characteristic for the occurrence of He II reionization.

While the simulation was running, we stored the data required

to compute mock spectra along random sight lines through the simulation box, at many thousands of output times. The time interval between individual snapshots is of order of the light crossing time through the box. This fine sampling of the redshift evolution allows us to take into account the detailed evolution of the density, temperature and ionizing background. We impose the ionizing background $J_{\text{G+Q}}(\nu, z)$ from QSOs and galaxies as computed by Haardt & Madau (1996) and updated by Haardt & Madau (2002⁸), but reduced in amplitude by a factor of j . Using $j = 2.75$ for all redshifts $2.5 \leq z \leq 4$ reproduces the observed evolution of $\bar{\tau}_{\text{eff}}$ quite well. This UV-background is different from the one used during the simulation. However, because the hydrogen gas is in photoionisation equilibrium, and because the hydrogen photo-heating rate is independent of the

⁸<http://pitto.mib.infn.it/~haardt/cosmology.html>

hydrogen ionizing flux, such a rescaling works accurately (see Theuns et al. 1998).

Using the mock spectra, we determine the evolution of $\bar{\tau}_{\text{eff}}$, binned in redshift intervals of order $\Delta z = 0.1$, and use bootstrap re-sampling to estimate the expected variance for the SDSS sample, given the number of QSOs available. This scatter could be underestimated due to missing large scale power in the simulation box, but such a systematic effect is unlikely to affect the relative decrement during and away from He II reionization.

In Fig. 1, we compare the evolution of T and $\bar{\tau}_{\text{eff}}$ in the two simulations, in which He II reionisation starts at redshifts 3.4 and 3.2, respectively. The temperature T increases suddenly by a factor ~ 1.8 following reionization. The effect of this temperature increase on $\bar{\tau}_{\text{eff}}$ is shown in the bottom panel. Away from He II reionization, $\bar{\tau}_{\text{eff}} \propto (1+z)^\zeta$, with $\zeta \approx 3.8$. The bottom panel of the figure shows the deviation from this scaling, $\bar{\tau}_{\text{eff}}/(1+z)^\zeta$, and illustrates that the temperature increase leads to a ≈ 10 percent decrease in $\bar{\tau}_{\text{eff}}$. After $\Delta z \approx 0.4$, $\bar{\tau}_{\text{eff}}$ recovers to the power-law evolution.

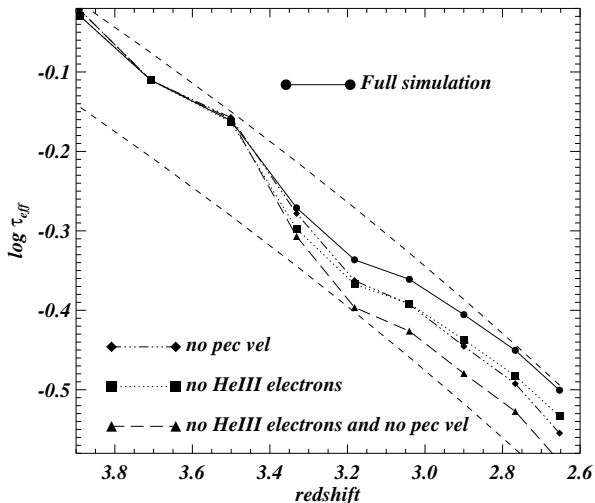


FIG. 2.— Evolution of $\bar{\tau}_{\text{eff}}$ for the simulation with He II reionization at redshift 3.4 (circles). The other curves illustrate two reasons why the change in effective optical depth is smaller than naively expected. If peculiar velocities are neglected in the computation of the spectra (diamonds), then the mean absorption is higher because gravitationally induced peculiar velocities tend to increase blending, which in turn decreases the opacity. The curve has been offset vertically to match the full simulation curve above $z = 3.5$. During He II reionization, pressure induced peculiar velocities push gas out of the filaments into the voids, and this increases the absorption, and consequently the two curves start to deviate. This shows that pressure induced peculiar velocities partly counteract the decrease in $\bar{\tau}_{\text{eff}}$. The increased electron density following He II reionization, neglected in computing the dotted curve (squares), has a similar effect on $\bar{\tau}_{\text{eff}}$. When both peculiar velocities and extra electrons are neglected (dashed curve connecting triangles), then the decrease in $\bar{\tau}_{\text{eff}}$ is $\approx (1/1.54^{0.7})$ (parallel dashed lines), close to that expected from the temperature dependence of the recombination coefficient.

This decrease is less than the $1/1.8^{0.7} \approx 30$ per cent naively

expected from the temperature dependence of the hydrogen recombination coefficient. Note however, that $\bar{\tau}_{\text{eff}}$ does not scale linearly with the optical depth, since $\exp(-\bar{\tau}_{\text{eff}}) = \langle \exp(-\tau) \rangle$, and that some of the absorbing gas is at densities higher than the mean, for which the relative change in temperature is less (Schaye et al. 2000). In addition, there are two other physical effects that lessen the dependence of $\bar{\tau}_{\text{eff}}$ on T . The extra electrons liberated during He II reionization tend to increase the neutral hydrogen abundance (Eq.3). For full He II reionization, the increase in $\bar{\tau}_{\text{eff}}$ is ≈ 7.5 per cent. Another effect is that the

filaments start to expand due to the extra heating (see Theuns, Schaye and Haehnelt, 2000, Fig (4)). These extra peculiar velocities also partly counteract the decrease in $\bar{\tau}_{\text{eff}}$. Both effects are illustrated in Fig. 2.

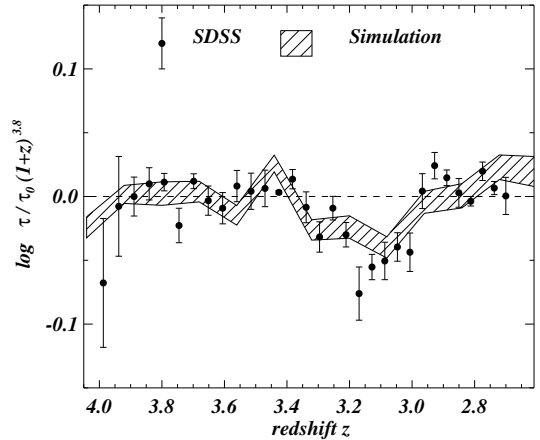


FIG. 3.— Deviation of the effective optical depth from a power-law evolution, $\bar{\tau}_{\text{eff}}/(1+z)^{3.8}$, for the SDSS data smoothed on 3000 km s^{-1} (symbols with error bars) and a hydrodynamical simulation of a ΛCDM model, in which He II reionization starts at $z = 3.4$ (hatched region). The errors in the SDSS data are determined from bootstrap re-sampling the individual spectra. The hatched region for the simulation delineates the 20 and 80 per centile of bootstrap re-sampled mock samples. The temperature increase associated with He II reionization causes $\bar{\tau}_{\text{eff}}$ to drop below the power-law evolution in the simulation. This characteristic dip matches very well the feature detected in the SDSS data.

3. DETERMINATION OF THE $\text{Ly}\alpha$ EFFECTIVE OPTICAL DEPTH IN THE SDSS DATA

Bernardi et al. (2002) determine $\bar{\tau}_{\text{eff}}(z)$ from 1061 moderate resolution ($\lambda/\Delta\lambda \approx 1800$) and intermediate signal-to-noise ratio (typically between 4 and 10) spectra of QSOs with redshifts between 2.75 and 4.3, color selected from the SDSS (Fig. 3). There are several crucial steps in the determination of the mean absorption from these spectra, such as the determination of the shape and amplitude of the continuum in each QSO spectrum, and assessment of possible biases introduced by the QSO selection criterion employed by the SDSS.

Full details of the procedure can be found in Bernardi et al (2002). Briefly, the shape of the continuum in the $\text{Ly}\alpha$ forest region is determined by solving simultaneously for the evolution of the effective optical depth and for the shape of the mean continuum, while allowing for the possibility that neither are well-fit by featureless power-laws. This is possible, because the (intrinsic) shape of a quasar's continuum is a function of *rest-frame* wavelength, whereas $\bar{\tau}_{\text{eff}}$ is measured at given *observed* wavelength. Two different methods were used, a χ^2 technique, and an iterative fitting procedure, and they give results in very good agreement with each other. Both techniques allow one to take into account the presence of weak emission lines in the QSO's continuum, and of deviations in the evolution of the optical depth from a smooth power-law.

Bernardi et al. present many tests of their methods. For example, they show that the scatter of individual measurements from the mean evolution is uncorrelated with rest-frame wavelength, which is not the case when the weak emission lines are not taken into account. The evolution of $\bar{\tau}_{\text{eff}}$ determined from

the SDSS data is consistent with previous measurements, and the excellent statistics allow for the detection of a localized feature in $\bar{\tau}_{\text{eff}}(z)$ of the order of 10 per cent. The next section compares the SDSS data to the hydrodynamical simulation.

4. RESULTS

The deviation of $\bar{\tau}_{\text{eff}}$ from a power-law $\bar{\tau}_{\text{eff}}/(1+z)^{3.8}$ is plotted in Fig. 3 for the SDSS sample (symbols with error bars) and the simulation for which He II reionization starts at $z \approx 3.4$ (hashed region). With respect to the power-law, the measured $\bar{\tau}_{\text{eff}}$ shows a distinctive dip around redshift $z = 3.14 \pm 0.03$ of depth $\Delta\bar{\tau}_{\text{eff}} = -0.09 \pm 0.02$ and width $\Delta z = 0.09 \pm 0.02$ (see Bernardi et al. 2002 for the determination of the errors), consistent with the signature of He II reionization. The similarity between the data and the simulation is striking. Note that the parameters for the simulation were tuned to match the temperature evolution measured by Schaye et al. (2000), and hence the dip in $\bar{\tau}_{\text{eff}}$ is a prediction of the model. The fact that the power-law evolution as measured from the SDSS is the same as computed from the simulation, suggests that the ionizing background $J_{\text{G+Q}}(\nu, z)$ describes the evolution of the photoionization rate well.

The amplitude, shape and duration of the deviation of $\bar{\tau}_{\text{eff}}/(1+z)^{\zeta}$ from a straight line is very similar for the SDSS data and the hydrodynamical simulation. The onset of the decrease in $\bar{\tau}_{\text{eff}}$ is not correctly modeled in the simulation, because the UV-background is assumed to be uniform at all times and because the rise in the UV-background does not take into account that photons are consumed during the reionization process. This is partly counteracted by the still relatively poor sampling $\Delta z \sim 0.1$ – worse than in the SDSS data – of the simulation outputs, but better sampling would show a much more rapid decrease in $\bar{\tau}_{\text{eff}}$ in the simulations. In reality, the temperature distribution will become inhomogeneous, as some regions become ionized – and hence hot – before others do. The spatial scale of these fluctuations is of the order of the size of a new He III region in a singly ionized and homogeneous He II Universe (Miralda-Escudé, Haehnelt & Rees 2000)

$$R = \frac{16.8}{1+z} \left(\frac{\dot{N}_{\text{ph}}}{10^{56} \text{s}^{-1}} \frac{t_{\text{QSO}}}{10^7 \text{yr}} \left(\frac{\Omega_b h^2}{0.02} \right)^{-1} \right)^{1/3} \text{Mpc}, \quad (5)$$

REFERENCES

Abel, T. & Haehnelt, M. G. 1999, ApJ, 520, L13
 Bahcall, J. N. & Salpeter, E. E. 1965, ApJ, 142, 1677
 Bernardi M. et al., 2002, submitted to AJ, preprint (astro-ph/0206293)
 Bryan, G. L. & Machacek, M. E. 2000, ApJ, 534, 57
 Bi, H. & Davidsen, A. F. 1997, ApJ, 479, 523
 Cen, R. & Bryan, G. L. 2001, ApJ, 546, L81
 Cen, R., Miralda-Escudé, J., Ostriker, J. P., Rauch, M., 1994, ApJ, 437, L9
 Couchman, H. M. P., Thomas, P. A., & Pearce, F. R. 1995, ApJ, 452, 797
 Davé, R., Hellsten, U., Hernquist, L., Katz, N., & Weinberg, D. H. 1998, ApJ, 509, 661
 Efstathiou, G., Schaye, J., & Theuns, T. 2000, Royal Society of London Philosophical Transactions Series, 358, 2049
 Gnedin, N. Y. 2000, ApJ, 535, 530
 Gunn, J. E. & Peterson, B. A. 1965, ApJ, 142, 1633
 Haardt, F. & Madau, P. 1996, ApJ, 461, 20
 Heap, S. R., Williger, G. M., Smette, A., Hubeny, I., Sahu, M. S., Jenkins, E. B., Tripp, T. M., & Winkler, J. N. 2000, ApJ, 534, 69
 Hernquist, L., Katz, N., Weinberg, D.H., Miralda-Escudé, J., 1996, ApJ, 457, L51
 Kim T-S, Cristiani S, D'Odorico S, 2002, A&A, in press, preprint (astro-ph/astro-ph)
 Kriss, G. A. et al. 2001, Science, 293, 1112
 Lynds, R. 1971, ApJ, 164, L73
 Machacek, M. E., Bryan, G. L., Meiksin, A., Anninos, P., Thayer, D., Norman, M., & Zhang, Y. 2000, ApJ, 532, 118
 Miralda-Escudé, J. & Rees, M. J. 1994, MNRAS, 266, 343
 Miralda-Escudé, J., Cen, R., Ostriker, J. P., Rauch, M., 1996, ApJ, 471, 582
 Miralda-Escudé, J., Haehnelt, M., & Rees, M. J. 2000, ApJ, 530, 1
 Mücke, J. P., Petitjean, P., Kates, R. E., & Riediger, R. 1996, A&A, 308, 17
 Peebles PJE, 1993, Principles of Physical Cosmology, Princeton University Press
 Reimers, D., Kohler, S., Wisotzki, L., Groote, D., Rodriguez-Pascual, P., & Warmsteker, W., 1997, A&A, 327, 890
 Ricotti, M., Gnedin, N. Y., & Shull, J. M. 2000, ApJ, 534, 41
 Schaye, J. 2001, ApJ, 559, 507
 Schaye, J., Theuns, T., Leonard, A., & Efstathiou, G. 1999, MNRAS, 310, 57
 Schaye, J., Theuns, T., Rauch, M., Efstathiou, G., & Sargent, W. L. W. 2000, MNRAS, 318, 817
 Smette, A., Heap, S. R., Williger, G. M., Tripp, T. M., Jenkins, E. B., & Songaila, A. 2002, ApJ, 564, 542
 Sokasian, A., Abel, T., & Hernquist, L. 2002, MNRAS, 332, 601
 Songaila, A. & Cowie, L. L. 1996, AJ, 112, 335
 Theuns, T., Leonard, A., Efstathiou, G., Pearce, F. R., & Thomas, P. A. 1998, MNRAS, 301, 478
 Theuns, T., Schaye, J., & Haehnelt, M. G. 2000, MNRAS, 315, 600
 Theuns, T., Zaroubi, S., Kim, T., Tzanavaris, P., & Carswell, R. F. 2002a, MNRAS, 332, 367
 Theuns, T., Schaye, J., Zaroubi, S., Kim, T., Tzanavaris, P., & Carswell, R. F. 2002b, ApJ, 567, L103
 Zaldarriaga, M. 2002, ApJ, 564, 153
 Zhang, Y., Anninos, P., Norman, M.L., 1995, ApJ, 453, L57

which corresponds to $\approx 1200 \text{ km s}^{-1}$ or $\Delta z = 0.016$ at redshift 3 (\dot{N}_{ph} is the luminosity of the QSO in ionizing photons, and t_{QSO} its age). Simulations that include radiative transfer and can resolve the Ly α -forest are required to model this process more realistically.

In principle, it should be possible to detect the onset of He II reionization from the occurrence of such ionized, hot He III bubbles. (The ‘thermal proximity effect’.) Theuns et al’s (2002b) wavelet method did not detect such temperature fluctuations on scales larger than 5000 km s^{-1} . However, they only attempted to identify *individual* He III regions, and did not quantify whether the presence of such hotter regions can be detected statistically. Zaldarriaga (2002) attempted to do just that, using the spectrum of QSO 1422+231, but again no signal was detected. With more data available now, such a detection may be possible.

In summary: the evolution of the effective optical depth $\bar{\tau}_{\text{eff}}$, measured in the SDSS quasar sample by Bernardi et al. (2002), deviates suddenly by ≈ 10 per cent at redshift $z \approx 3.1$ from a smooth power-law. The mean absorption determined from a hydrodynamical simulation of the IGM, in which He II reionization starts at redshift 3.4, provides an excellent match to this feature in $\bar{\tau}_{\text{eff}}$. In this simulation, the decrease in absorption is due to the temperature dependence of the hydrogen recombination coefficient, and the required temperature change due to He II reionization, is in good agreement with the temperature measurements from Schaye et al. (2000) and Theuns et al. (2002). We consider this strong evidence that He II reionization has been detected in the SDSS data. The onset of reionization starts around $z \sim 3.4$ and percolation, corresponding to the maximum deviation of $\bar{\tau}_{\text{eff}}$ from a power-law, occurs at $z \sim 3.1$.

Acknowledgments TT thanks PPARC for the award of an Advanced Fellowship. JS is supported by a grant from the W.M.Keck Foundation. This research was conducted in cooperation with Silicon Graphics/Cray Research utilizing the Origin 2000 super computer at the Department of Applied Mathematics and Theoretical Physics in Cambridge.